Simultaneous Analysis of Seismicity Rate Change and Quiescence in the Thailand-Laos-Myanmar Borders: An Updated Prospective Earthquake Source

Manunchaya Neanudorn and Santi Pailoplee*

Morphology of Earth Surface and Advanced Geohazards in Southeast Asia Research Unit (MESA RU), Department of Geology, Faculty of Science, Chulalongkorn University, Bangkok 10330, Thailand
*Corresponding author e-mail: Pailoplee.S@gmail.com

Received: 10 Apr 2022
Revised: No revision
Accepted: 25 Apr 2022

ABSTRACT

To investigate the precursory seismic quiescence associated with upcoming hazardous earthquakes, seismicity data collected in the vicinity of the Thailand-Laos-Myanmar borders were analyzed using the seismicity rate change (Z-value) technique and the Region-Time-Length (RTL) algorithm, which were chosen for this study based on previous successful investigations. The Thailand Meteorological Department provided the seismic data used in this study. Following that, the catalog's homogeneity and completeness were improved. Nineteen case studies of strong-to-major earthquakes were examined retrospectively, but the results of six connected occurrences using two methods were chosen. After performing iterative tests on the seismicity rate change using different values of N_w = 25 and T_w = 1.5, as well as the RTL algorithm parameters r_0 = 60 km and t_0 = 2.5 y, reasonable estimates of the anomalous Z-values and RTL scores a few years prior to major recognized earthquakes were obtained in both temporal variation and spatial distribution. Both the Z-value and the RTL algorithm identified almost the same potential regions for an approaching large earthquake: the northern part of Chiangmai, Thailand; the TLMB triple junction; and Mong Pan, Myanmar.

Keywords: Earthquake Catalogue; Precursory Seismic Quiescence; Seismicity rate change; Z-value; RTL Algorithm; Earthquake Forecasting.

1. INTRODUCTION

Pailoplee and Choowong (2014) identified the Thailand-Laos-Myanmar border as the intraplate seismotectonic setting in Mainland Southeast Asia, one of the most seismically active zones. While Pailoplee, Channarong, and Chutakositkanon (2013) studied seismic activity from 1984 to 2020, the Thailand Meteorological Department's earthquake catalogue shows large earthquakes occurred in this area. For example, an earthquake of M_w-6.8 on March 24th, 2011, in Tarlay, Myanmar (Wang et al., 2014), and a M_w-6.4 on November 21st, 2019, in northwest Laos near the Thai border may all be felt in Bangkok. The research results show that the spatial distribution of the b-value indicates the epicenter of the earthquake occurring around the lowest b-value area. As a result, the TLMB is now designated as a zone of high seismic activity (Figure 1).

According to Sobolev (1995), laboratory rock experiments revealed two distinct phases of seismicity rates prior to a major earthquake's rupturing process: the quiescent (seismicity decrease) and activation (seismicity increase) stages. Seismic quiescence is the most effective of these stages as a precursor and it has been

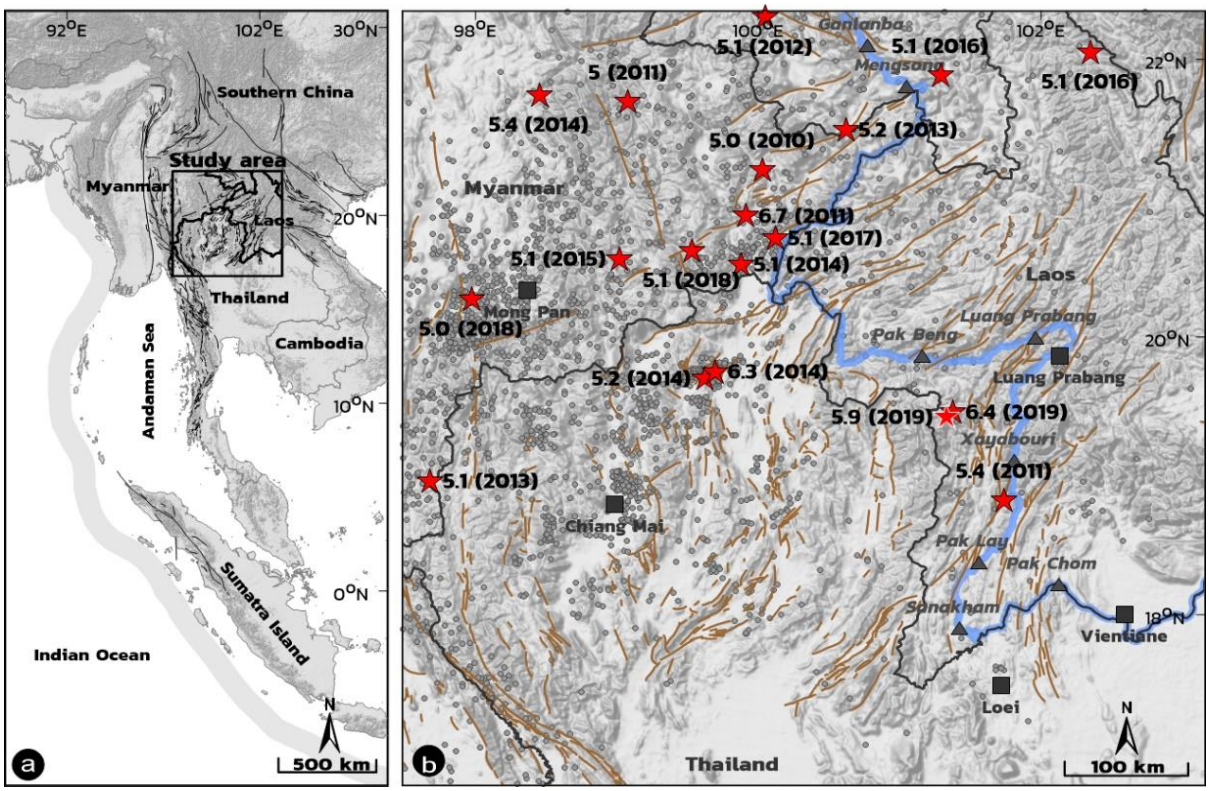

Figure 1. (a) Map of Thailand and neighboring countries indicating the area under study (box with black line). (b) Map displaying the distribution of complete seismicity catalogue epicenters (gray dots, containing all catalogues) and strong earthquake epicenters (red star, containing $M_w \geq 5.0$) along Thailand-Laos-Myanmar borders between 2010 and 2020. Fault lines, the Mae Kong River, hydropower dams, and major cities were represented by a brown line, a thick blue line, grey triangles, and grey squares, respectively.

successfully applied in earthquake forecasting over the past four decades. Several ideas have been proposed recently to identify earthquake precursors. Moreover, some significant investigations have reinforced the theory that seismic quiescence precedes large earthquakes (Katsumata, 2011).

Thus, a variety of statistical methods for earthquake forecasting have been demonstrated to determine the earthquake precursor, including the Z-value (Wiemer and Wyss, 1994) and the Region-Time-Length (RTL) algorithm (Sobolev and Tyupkin, 1997). The Z-value is one of the additional techniques for detecting the precursory seismic quiescence that occurs before strong-to-major earthquakes, such as the M_w-5.8 Coyote lake earthquake, USA and M_w-6.2 Morgan Hill earthquake (Bachman, 2001), The 2008 M_w-6.4 SW-Achaia, Western Greece (Chouliaras, 2009), the M_w-6.4 Turkey (Ozturk and Bayrak, 2009), The 2003 M_w-7.6 Colima earthquake, Mexico (Rudolf-Navarro et al., 2010), the 2003 Mw-8.3 Tokachi-oki, Japan (Katsumata, 2011), and the 2006 M_w-6.1 Silakhour, Iran (Sorbi et al., 2012)

Another successful forecasting tool for quantifying relative seismic quiescence is the RTL algorithm. A number of RTL investigations have revealed the successful correlation between the quiescent and activation stages and subsequent moderate-to-major earthquakes in various seismogenic settings, such as the M_w-7.2 Kobe earthquake, Japan (Huang et al., 2001), the M_w-6.8

Nemuro earthquake, Japan (Huang and Sobolev, 2002), the M_w-7.3 Izmit earthquake, Turkey (Huang et al., 2002), the M_s-7.3 Tottori earthquake, Japan (Huang and Nagao, 2002), earthquakes with $M_s \geq 5.0$ in northern China (Jiang et al., 2004), earthquakes with $M_s \geq 6.0$ in the Yunnan area (Liu and Su, 2006), M_w-7.3 Chi-Chi earthquake, Taiwan (Chen and Wu, 2006), M_s-8.0 Wenchuan earthquake, China (Huang, 2008), and the latest hazardous event of the M_w-9.0 Tohoku earthquake, Japan (Huang and Ding, 2012).

As mentioned previously, the purpose of this study was to validate the use of Z-value and the RTL algorithm to analyze seismicity rate change and quiescence along the TLMB region prior to the occurrence of nineteen hazardous earthquakes ($M_w \geq 5.0$), and then to determine the prospective areas of upcoming earthquakes along the TLMB using the most recent seismicity data. The findings should help constrain the potential locations of future earthquakes, as well as comparing the potential of the two methods of forecasting.

2. DATA IMPROVEMENT

We used the earthquake catalogue from the Thailand Meteorological Department (TMD) in this research. The earthquake records between 2007 - 2020 along the Thailand-Laos-Myanmar border (13.77º-25.35ºE and 94.48º-106.07ºN) were analyzed (Figure 2a). The magnitude class of the earthquake catalogue from TMD is moment magnitude (M_w). To determine completeness, we used Gardner and Knopoff (1974) approach to remove the foreshock and aftershock. In 2005, Woessner and Wiemer made a presumption called Entire-magnitude Range. We found that the magnitude of completeness (Mc) = 3.0 M_w between January 4th, 2007, and September 22nd, 2020, can cover most of the Thailand-Laos-Myanmar borders (Figure 2b).

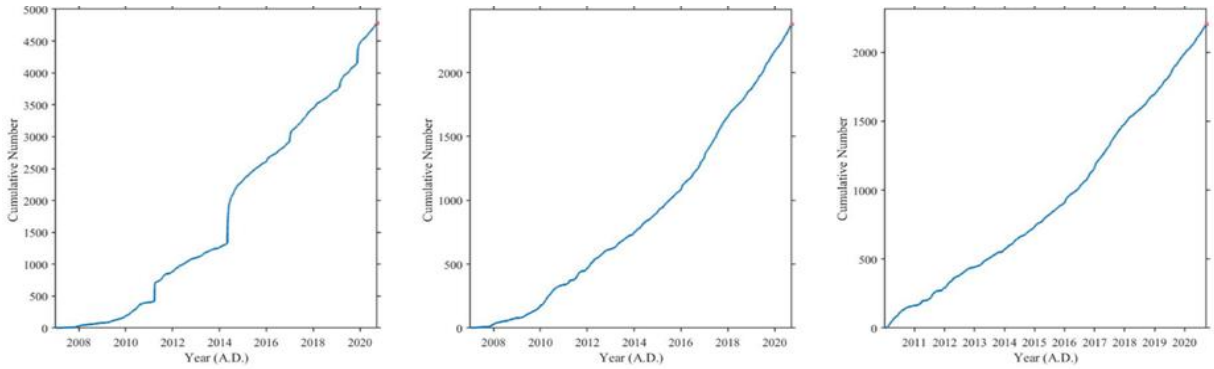

Figure 2. Cumulative number graph showing the rates of (a) seismicity detected from TMD during period 2007-2020, (b) the earthquake catalogue after declustering, (c) the completeness earthquake catalogue after the GENAS technique during January 6, 2010, and September 22, 2020.

Furthermore, using the GENAS technique (Habermann, 1983; 1987), this technique eliminated the harmonic main shock of the magnitude completeness. As seen in Figure 2b, there is no evidence of apparent man-made activity in the bulk seismicity rate, as noted by Wyss (1991) and Zuniga and Wiemer (1999). As a result, we chose to include all 2022 remaining major shocks with Mc ≥ 2 M_w observed between 2010 and 2020 in this Z-value and RTL investigation (Figure 2c).

3. SEISMICITY RATE CHANGE (Z-VALUE)

The Z-value, as described by Equation 1, was used in this work to evaluate the precursory seismic quiescence, which is a

decrease in seismicity induced prior to dangerous earthquakes (Wiemer and Wyss, 1944).

$$Z = \frac{R_{bg} - R_w}{\sqrt{\frac{s_{bg}^2}{N_{bg}} + \frac{s_w^2}{N_w}}}, \quad (1)$$

in where Z is the seismic quiescence rate, which is expressed by the difference between the average seismicity rate inside a certain time window (R_w) and the general period prior to the studied time frame (R_{bg}). In this equation, the parameters S_w and S_{bg} are defined as the standard deviations of R_w and R_{bg}, respectively, whilst the parameters N_w and N_{bg} are specified as the number of earthquakes. According to seismology, the positive and negative Z-value represent the quiescence and activation stages, respectively, during which the seismicity rate is less or greater than the background rate.

3.1 Temporal Investigation

In terms of temporal investigation, the free characteristic parameters included ($_i$) the number of earthquakes (N_w; 25-150 with 25 event intervals) and (ii) the time frame (T_w; 0.5-15 year with 0.5-year intervals) and the two were adjusted. The repeated test of 180 (6 × 30) characteristic variables found that N_w = 25 events and T_w = 1.5 year were the most appropriate characteristic parameters. Thirteen seismicity precursors were discovered during the retrospective temporal investigation of the nineteen strong-to-major earthquake occurrences. Due to a lack of seismicity data, the M_w-5.0, M_w-5.4, M_w-6.7, M_w-5.0, M_w-5.1, and M_w-5.1 earthquakes of 2010-2013, and M_w-5.1 of 2016 could not discover any anomalous Z-values prior to the earthquakes' occurrences (Table 1). The cumulative numbers of earthquakes versus time were shown for each case study (Figure 3). Following that, the Z-value was calculated using the long-term average function developed by Wiemer and Wyss (1994),

Table 1. The following is a list of strong-to-major earthquakes ($M_w \geq 5.0$) that occurred within the TLMB between 2010 and 2020, as well as the results from the Z-value investigation using N_w = 25 events and T_w = 1.5 y and the results from RTL algorithm investigation using r_0 = 60 km. and t_0 = 2.5 y.

No.	Longitude (ºN)	Latitude (ºE)	Date	Time (UTC)	Depth (km)	M_w	Z	Qs (A.D.)	Q-time (years)	RTL score	Qs (A.D.)	Q-time (years)
1	100.03	21.2	March 19, 2010	23:23	0	5	-	-	-	-	-	-
2	101.74	18.82	February 23, 2011	16:10	0	5.4	-	-	-	-	-	-
3	99.91	20.87	March 24, 2011	14:17	0	6.7	-	-	-	-	-	-
4	99.08	21.69	July 12, 2011	21:46	0	5	-	-	-	-	-	-
5	100.05	22.3	September 17, 2012	07:23	0	5.1	-	-	-	-	-	-
6	97.68	18.96	April 10, 2013	02:35	0	5.1	0.5	2011.7	2.9	-	-	-
7	100.62	21.49	September 22, 2013	23:44	10	5.2	2.3	2011.7	2	-0.61	2013.24	0.5
8	99.62	19.7	May 5, 2014	00:50	7	5.2	1.7	2012.78	1.6	-0.55	2014.04	0
9	99.692	19.748	May 5, 2014	11:19	7	6.3	2.2	2012.78	1.6	-0.56	2014.05	1
10	99.88	20.52	June 9, 2014	14:10	5	5.1	3	2011.24	3.2	-0.65	2013.74	0.7
11	98.45	21.74	December 26, 2014	17:31	10	5.4	1.1	2012.13	4.5	-0.65	2013.28	1.7
12	99.02	20.56	May 24, 2015	10:55	16	5.1	2.2	2010.98	4.4	-0.72	2012.85	2.3
13	101.29	21.88	March 5, 2016	12:20	10	5.1	2	2014.12	2.1	-	-	-
14	102.35	22.05	April 22, 2016	01:38	20	5.1	-	-	-	-	-	-
15	100.12	20.71	April 18, 2017	19:42	2	5.1	4.7	2013.78	6.7	-0.26	2013.74	3.6
16	99.53	20.62	February 3, 2018	15:31	5	5.1	4.3	2014.01	7.4	-0.24	2013.08	4.4
17	97.97	20.27	July 1, 2018	20:42	2	5	2.9	2011.59	6.9	-	-	-
18	101.376	19.456	November 20, 2019	00:02	3	6.4	4.4	2015.42	7.9	-0.08	2013.55	6.3
19	101.333	19.421	November 20, 2019	21:19	5	5.9	4.7	2015.42	7.9	-0.08	2013.55	6.3

The parameters Z, RTL Score, Qs, and Q-time indicate, the minimum RTL score, the maximum Z-value, starting time of the defined seismic quiescence and the time span between the quiescence and the occurrence time of the earthquake, respectivel

as shown in Equation 1. Because this research focuses on the comparison of Z-values and RTL algorithms, we will discuss just the case studies that are related, specifically with case study nos. 8, 9, 10, 12, 15, and 16.

The next paragraph contains the findings of the retrospective temporal research. Figure 3a shows a maximum Z-value of 1.7 in 2012.78, followed by a 5.2 M_w earthquake on May 5th, 2014, northeast of Chiang Mai, Thailand. In Figure 3b, the greatest Z-value is 2.2 in 2012.78, and then 1.6 years later, on May 5th, 2014, a 5.2 M_w earthquake struck northeast of Chiang Mai, Thailand. Figure 3c shows a maximum Z-value of 3 at 2012.82 and then an M_w-5.1 earthquake on June 9th, 2014, east of Mong Pan, Myanmar. In Figure 3d, the computed Z-value depicts the 2012.13 peak (Z = 1.1). Following that, 4.4 years later, on May 24th, 2015, an M_w-5.1 earthquake occurred east of Mong Pan, Myanmar. (See No. 12 in Table 1). For Figure 3e, the highest Z-value of 4.7 occurs in 2013.78, and then, around 6.7 years later, the M_w-5.1 earthquake struck eastern Mong Pan, Myanmar, on April 18th, 2017. (See No. 15 in Table 1). The determined Z-value in Figure 3f depicts the peak (Z = 4.7) at 2014.01. Following that, approximately 7.4 years later, on Feb 3th, 2018, an M_w-5.1 earthquake struck eastern Mong Pan, Myanmar. (See No. 16 in Table 1).

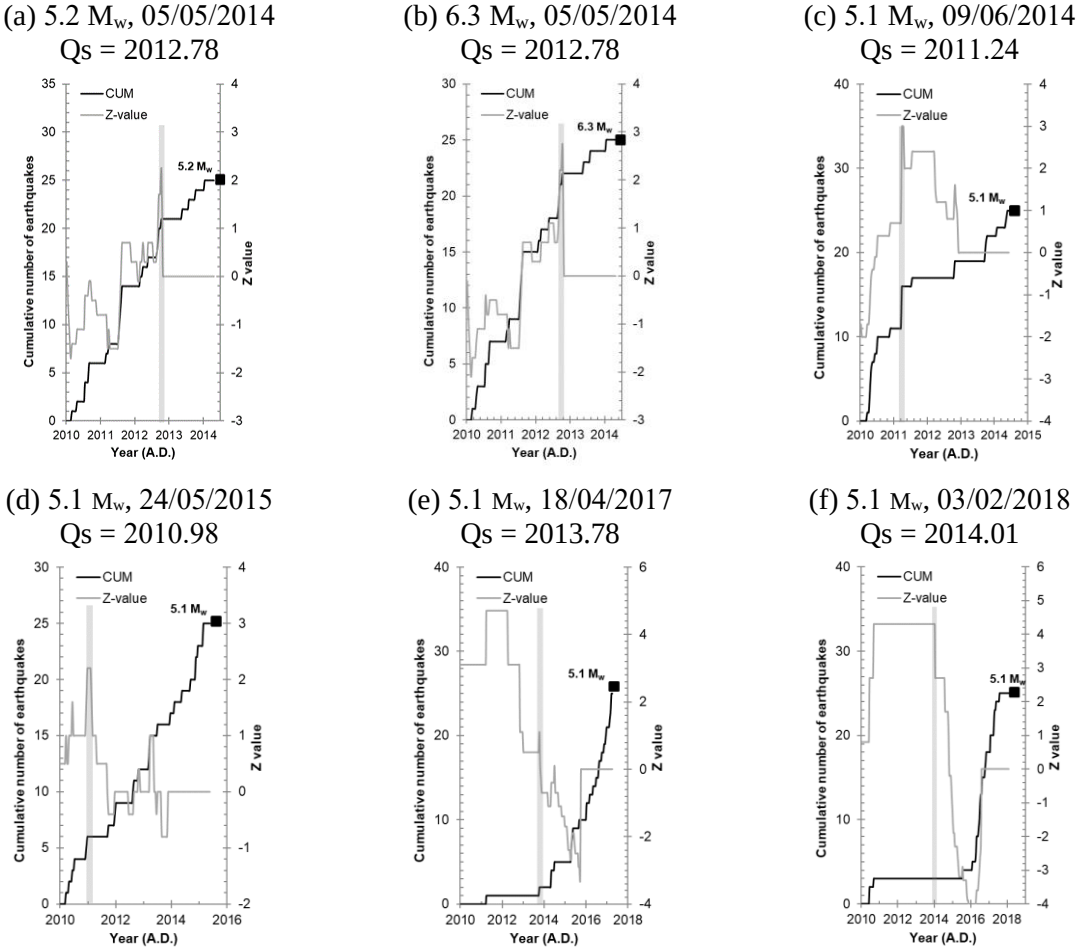

Figure 3. (a-f) Grpah plot between the cumulative number of earthquakes (grey line) and Z-value (black line) are plotted against time. The black stars indicate the time of each earthquake's occurrence. The transparent grey strip illustrates the Z-value anomaly, which is recognized as the quiescence stage.

3.2 Spatial Investigation

The potential Z-value for identifying earthquake precursors in the TLMB region was explored spatially and mapped in order to restrict the potential Z-value for detecting earthquake precursors in the region. The TLMB region was gridded using cells with a dimension of 0.25° x 0.25°, the nearest 50 events from the earthquake data were found in each individual grid node, and the Z-value was derived spatially in the same method as in the prior temporal investigation. The Z-value of each grid node was picked, contoured, and mapped in accordance with the previously stated quiescence time (Figure 3 in column Qs in Table 1), and the resulting maps of thirteen samples are given in Figure 4.

The spatial distribution of the Z-value investigated in 2012.78 and 2012.78 (Figures 4a and 4b) indicated a larger Z anomaly that was scattered in three areas: western Mong Pan, Myanmar; northern Chiangmai, Thailand; and western Luang Prabang, Laos. Then, on May 5th, 2014, 5.2 and 6.3 years later, earthquakes, respectively, struck northeast of Chiangmai, Thailand, inside the highest Z anomaly area mentioned before (Nos. 8-9 in Table 1). In 2011.24 (Figure 4c), the spatial distribution of the Z-value indicated a more noticeable

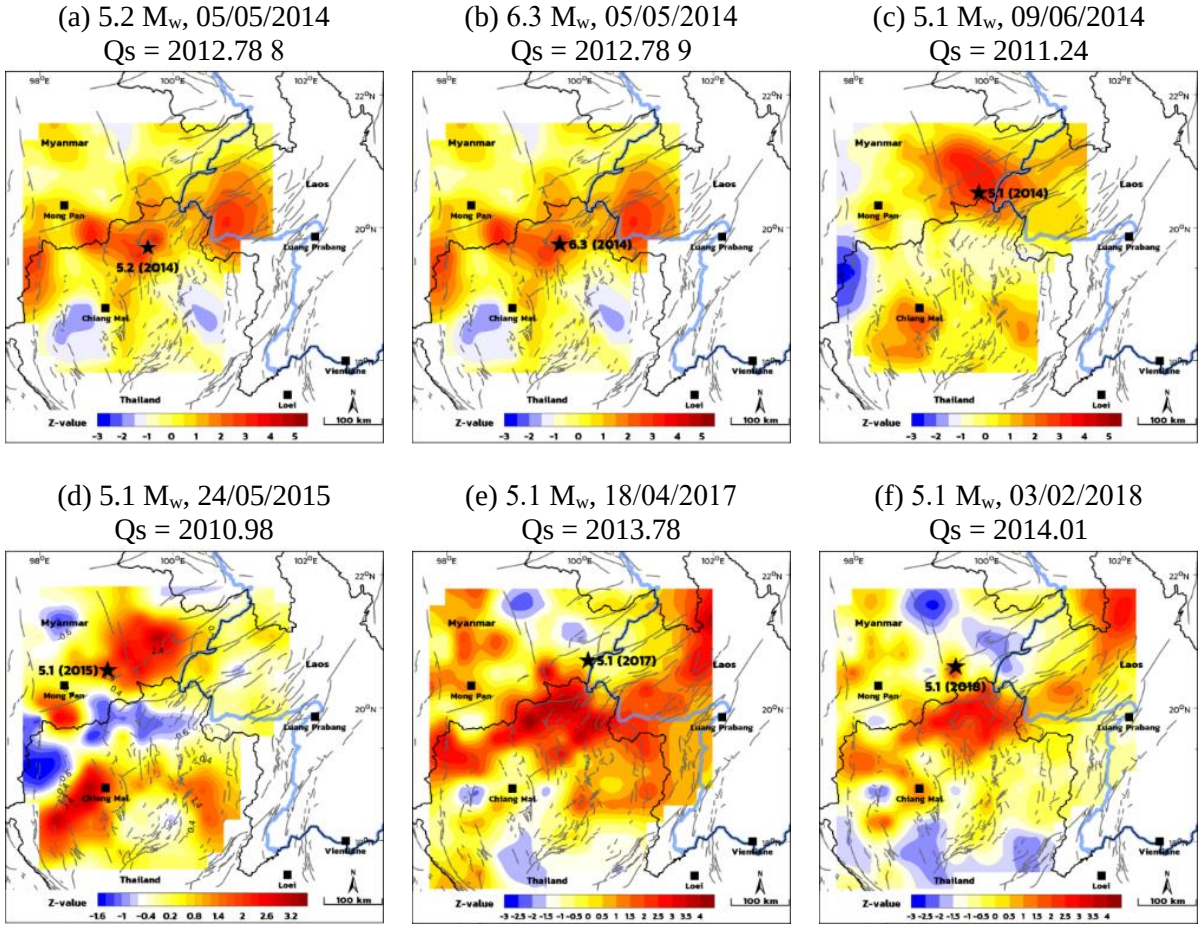

Figure 4. The spatial distribution of a-m the Z-values for thirteen of nineteen large earthquakes (numbers 6-13, 15-19 in Table 1) during the time slice of seismic quiescence determined from the temporal investigation are depicted on a map of the TLMB (Figure 3). The colors red and blue represent a decrease (+Z) and an increase (-Z) in seismicity rate, respectively. Black stars show the epicenter of the earthquake case study.

Z anomaly that was scattered in two parts: along the TLMB boundary and Chiangmai, Thailand, near where the greatest Z anomaly region was displayed above. This spatial distribution of the Z-value is related to a 5.1 magnitude earthquake (No.10 in Table 1). In 2010.98 (Figure 4d), an anomalous Z-value was distributed west of the TLMB boundary and around Chiangmai, Thailand. Following that, about 4.4 years later, the epicenter of the M_w-5.1 earthquake that occurred on May 24th, 2015 (No. 12 in Table 1) was located east of Mong Pan, Myanmar, along the rim of the positive Z anomalies with a Z-value of 2.2. Figure 4e shows the Z map for 2013.78. It shows that an anomalous Z-value was spread from NW to SE over northern Thailand and northern Laos. After around 6.7 years, the epicenter of the M_w-5.1 earthquake that occurred on April 18th, 2017 (No. 15 in Table 1) was discovered east of Mong Pan, Myanmar, on the rim of the Z anomalies with a positive Z-value of 4.7. An anomalous Z-value was spread in a NW-SE direction throughout northern Thailand and northern Laos for the Z map in 2013.78 (Figure 4f). Following that, the epicenter of the M_w-5.1 earthquake that occurred on February 3rd, 2018 (No. 16 in Table 1) was situated around 7.4 years later to the east of Mong Pan, Myanmar, on the rim of the Z anomalies with a positive Z-value of 4.3. (Figure 4f).

4. SEISMIC QUIESCENCE (RTL ALGORITHM)

The RTL algorithm (Sobolev and Tyupkin, 1997; 1999) is a useful method of statistical seismology that was developed to detect the presence of precursory seismicity changes associated with the occurrence of the main shock (Sobolev 1995). The RTL algorithm weights three parameters called as R (interested region), T (time), and L (rupture length), which can be expressed as the following Equations 2-4:

$$R(x,y,z,t)=\left[\sum_{i=1}^{n}\exp\left(-\frac{r_i}{r_0}\right)-R_{bg}(x,y,z,t)\right] \quad (2)$$

$$T(x,y,z,t)=\left[\sum_{i=1}^{n}\exp\left(-\frac{t-t_i}{t_0}\right)-T_{bg}(x,y,z,t)\right] \quad (3)$$

$$L(x,y,z,t)=\left[\sum_{i=1}^{n}\exp\left(-\frac{l_i}{r_i}\right)-L_{bg}(x,y,z,t)\right] \quad (4)$$

Where (x, y, z, t) indicate the investigation location and time, and r_i indicates the distance between (x, y, z) and the epicenter of the i_{th} earthquake. Meanwhile, t_i and li are the origin time and length of the earthquake's surface fault rupture, respectively, which are proportional to the earthquake's magnitude (Mi) (Wells and Coppersmith 1994). R_{bg} (x, y, z, t), T_{bg} (x, y, z, t), and L_{bg} (x, y, z, t) define the background values of R (x, y, z, t), T (x, y, z, t), and L(x, y, z, t), respectively, whereas r_0 and t_0 define the characteristic distance and time span, respectively. The parameter n represents the total number of earthquakes with a magnitude greater than the completeness magnitude (Mc; Woessner and Wiemer 2005). Meanwhile, $2r_0$ equals R_{max} r_i and $2t_0$ equals T_{max} t - t_i. The RTL score or VRTL (x, y, z, t) may be calculated using the R, T, and L in Equation 5.

$$V_{RTL}(x,y,z,t)=\frac{R(x,y,z,t)}{R(x,y,z,t)_{\max}}\bullet\frac{T(x,y,z,t)}{T(x,y,z,t)_{\max}}\bullet\frac{L(x,y,z,t)}{L(x,y,z,t)_{\max}} \quad (5)$$

After all, the RTL score is a numeric number ranging from -1 to 1. V_{RTL} = 0 implies the normal activity of the seismicity. Meanwhile, V_{RTL} < 0 and > 0 represent a seismic quiescence and activation, respectively. Moreover, the spatial distribution for RTL algorithm, Huang et al. (2002) developed the Q (x, y, z, t1, t2) function as Equation 6 to

measure the average of RTL values during the time window [t1, t2]

$$Q(x,y,z,t_1,t_2) = \frac{1}{m}\sum_{i=1}^{m} RTL(x,y,z,t_i) \quad (6)$$

Where m is the number of RTL data points in the window [t1, t2] (the RTL parameter is derived using equation (4), which is included in [t1, t2]. Figure 3 illustrates the algorithms that have been introduced.

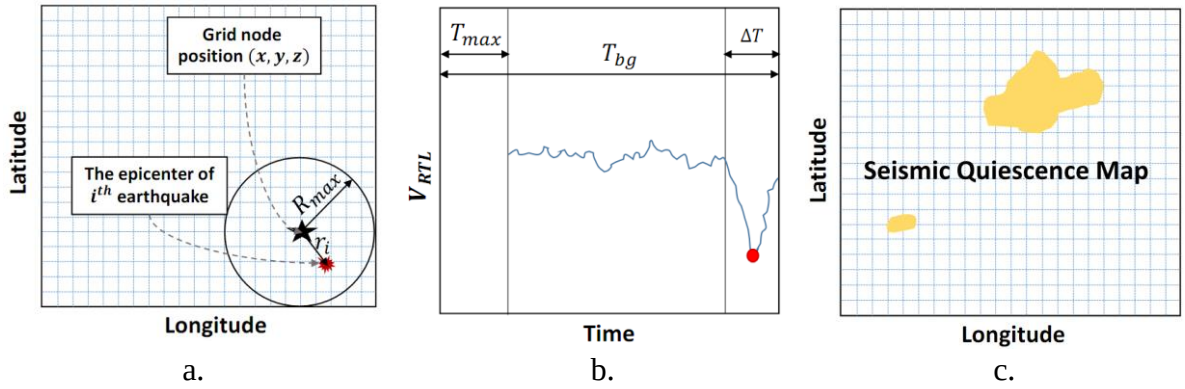

a. b. c.

Figure 5. The diagrams illustrating the spatial distribution of seismic quiescence at the position (x, y, z) show (a) the R_{max}-defined frame area threshold and the distance between the selected grid node and the ith earthquake's epicenter point. (b) The diagram illustrates the V_{RTL} curve at each grid node considered and the minimum V_{RTL} (indicated by a red circle), where T_{bg} denotes the total background time used to calculate the RTL algorithm, ΔT denotes the time span used to investigate seismic quiescence, and T_{max} denotes the time span with a restricted range. (c) An illustration of the seismic quiescence map. The shaded region denoted the research area's seismic quiescence throughout the period under consideration. (Puangjaktha and Pailoplee, 2016)

4.1. Temporal Investigation

The RTL algorithm was investigated retrospectively in both temporal and spatial aspects at the epicenters of nineteen strong-to-major earthquakes ($M_w \geq 5$) previously recorded within the TLMB in order to define the relationship between the RTL score and the subsequent occurrence of a hazardous earthquake at a given locality (Table 1). The result is a set of distinctive characteristics (r_0 and t_0, which are connected to R_{max} and T_{max}, respectively) that may be used to detect the precursory RTL score generated before to the dangerous earthquake in the TLMB. To do this, r_0 was altered between 50 and 200 km at 5-kilometer intervals, while t_0 was varied between 1 to 5 y at 0.5 y intervals. Thus, for each case study of an earthquake, 144 (16 × 9) situations of the distinctive parameters were examined repeatedly. The results showed that the characteristic distance r_0 of 60 km (R_{max} = 120 km) and time t_0 of 2.5 years (T_{max} = 5 years) were the most effective conditions for finding the anomalous RTL score connected to five of the eight detected earthquakes after repeated tests (Table 1). The RTL score was analyzed every 10 days the beginning of accessible seismicity data (2010) till the occurrence time of each earthquake examined in the retrospective temporal investigation. The temporal variations of the RTL score for the five successful case studies are shown in Figure 6. Due to the fact that this research compares Z-values and RTL methods, we will cover just those case studies

that are relevant, namely case studies 8, 9, 10, 12, 15, and 16.

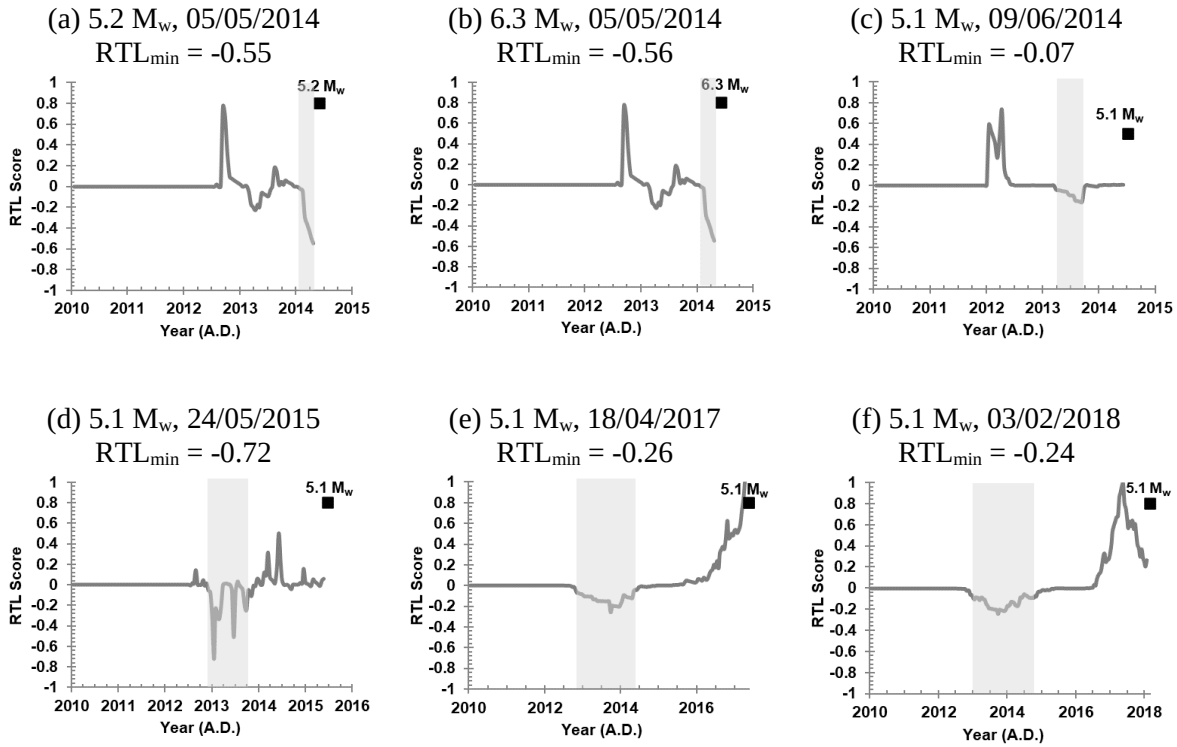

Figure 6. Temporal variation of the RTL score (grey line) of six strong-to-major earthquakes. Strong-major earthquakes are depicted by the black square.

Figure 6a shows the temporal variations in the RTL score at the location of the M_w-5.0 earthquake, revealing the activation stage began in 2012.70. Following that, the RTL score dropped sharply, reaching the first stage of quiescence in 2013.35. On the other hand, the RTL curve exhibits a little variation for 0.5 years until the second quiescence stage, with the lowest RTL score in 2014.31 (RTL score =-0.55). On the other hand, the earthquake occurred during the quiescent state. The similarity in Figures 6a and 6b might be due to the fact that the earthquakes in the case study happened at a similar time and location. By the beginning of the activation stage in 2012.62, the RTL score then dropped sharply, reaching the first stage of quiescence in 2013.28. The RTL curve displays a little variation for 0.5 years before the second quiescence, with the lowest RTL score in 2014.31 (RTL score = -0.56). On the other hand, the 6.3 M_w earthquake happened during a quiescent state. The RTL score at the location of the M_w-5.1 earthquake on June 9th, 2014 (Figure 6c) was stable between 2010.09 and 2010.93. The RTL score increased sharply to two activation stages in 2012.25 and 2012.28, but then the score decreased to a quiescence stage in 2012.32-2012.74. The RTL score finally reached the lowest level in 2013.70 (RTL score = -0.07). In Figure 6c, the RTL score curve clearly indicates three quiescent stages (i.e., 2012.85-2013.24, 2013.39-2013.51, and 2013.58-2013.78) and two activation stages (i.e., 2014.12-2014.24 and 2014.31-2014.66). From the minimum RTL score (-0.72), the quiescent stage of 2012.85-2013.24 was defined as the precursor of the M_w-5.1 main shock on May 24th, 2015). The RTL score curve in Figure 6d clearly demonstrates three quiescent periods (2012.85-2013.24, 2013.39-2013.51, and 2013.58-2013.78) and two activation stages (i.e., 2014.12-2014.24 and 2014.31-2014.66).

After the activation stage, the RTL curve has a small variant for 1 y before the occurrence of M_w-5.1 major shock on May 24th, 2015. The quiescent stage of 2012.85-2013.24 was determined as the precursor of this event based on the minimal RTL score (-0.72). According to Figure 6e, seismic quiescence began to decline in 2012.78 and peaked in 2013.74 (RTL score = - 0.26). Additionally, the RTL score suggests an activation stage between 2015.81 and 2017.21, with a maximum RTL score of 0.40, although the April 18th, 2015, 6.3 M_w earthquake occurred during an activation stage. Finally, the variation in the RTL score demonstrated the seismic quiescence clearly in Figure 6f. The RTL began dropping in 2013.08 and reached - 0.24 in 2013.24, before gradually reverting to the background rate in 2014.96. Following that, the RTL score indicated an activation stage between 2016.61 and 2017.99, with a maximum RTL score of 0.96; nevertheless, the February 3rd, 2015, 5.1 M_w earthquake happened during this time.

4.2. Spatial Investigation

To re-evaluate the RTL algorithm's suitability for earthquake forecasting, the RTL score was further evaluated spatially. To begin, the study area (Figure 1) was gridded using a grid interval spacing of 0.25 x 0.25. The temporal variation of the RTL score was determined at each grid node using Equations 1-4. The Q parameter (Huang 2004) was used to spatially map the RTL score, as described in Equation 5; for each grid node, the Q parameter was computed, contoured, and mapped as shown in Figure 7.

For instance, in Figure 7a, the distribution of the Q parameter averaged for the time period 2014.04-2014.31 reveals seismic quiescence in two areas covering approximately 200 km^2 north of Chiang Mai, Thailand. The epicenter of the M_w-5.2 earthquake that struck on May 5th, 2014, occurred within the rim of the minimum RTL score location. The similarities between Figures 7a and 7b might be because of the comparable time and place of the earthquakes. Figure 7b displays the Q parameters for the time period 2014.04-2014.31, during which an anomaly was formed in a 200 km^2 region north of Chiang Mai, Thailand. The M_w-6.3 earthquake that struck on May 5th, 2014, occurred northeast of Chiangmai, Thailand. It occurred along the rim, which is where the minimal RTL area is located. The quiescent time calculated from temporal research for the 5.1 M_w earthquake that struck east of Mong Pan, Myanmar, along the TLMB boundary, was in the range of 2013.35-2013.74, with the spatial distribution of the RTL score shown in Figure 7c. In the area of Mong Pan Myanmar, there were several quiescent anomalies. The earthquake's epicenter, on the other hand, was in the eastern part of the anomaly. In Figure 7d, covering the quiescent period of 2012.85-2013.24, a prominent anomaly occurred in two portions: a weak anomaly in Chiangmai, Thailand, and a strong anomaly in the north of Mong Pan, Thailand. In addition, the epicenter of the 5.1 M_w earthquake that occurred on May 24th, 2015, was located in the rim the defined strong RTL anomalies (Figure 7d). Figure 7e illustrates an anomaly in two locations: a minor anomaly in the south of Chiangmai, Thailand, and a significant anomaly in the northeastern part of Mong Pan, Myanmar. Additionally, the epicenter of the 5.1 M_w April 18th, 2017, earthquake was located near the defined significant RTL anomalies (Figure 7e). Finally, as illustrated in Figure 7f, the spatial distribution of the RTL score from 2013.08 to 2014.96 demonstrated that the seismic quiescence area covered about 200 km^2 along the Myanmar-Laotian border. The lowest RTL score, in particular, denotes the northeastern section of Mong Pan, Myanmar. The epicenter of the 5.1 M_w earthquake that struck on February 3rd, 2018, was located in the southern portion of the RTL anomaly (Figure 7f).

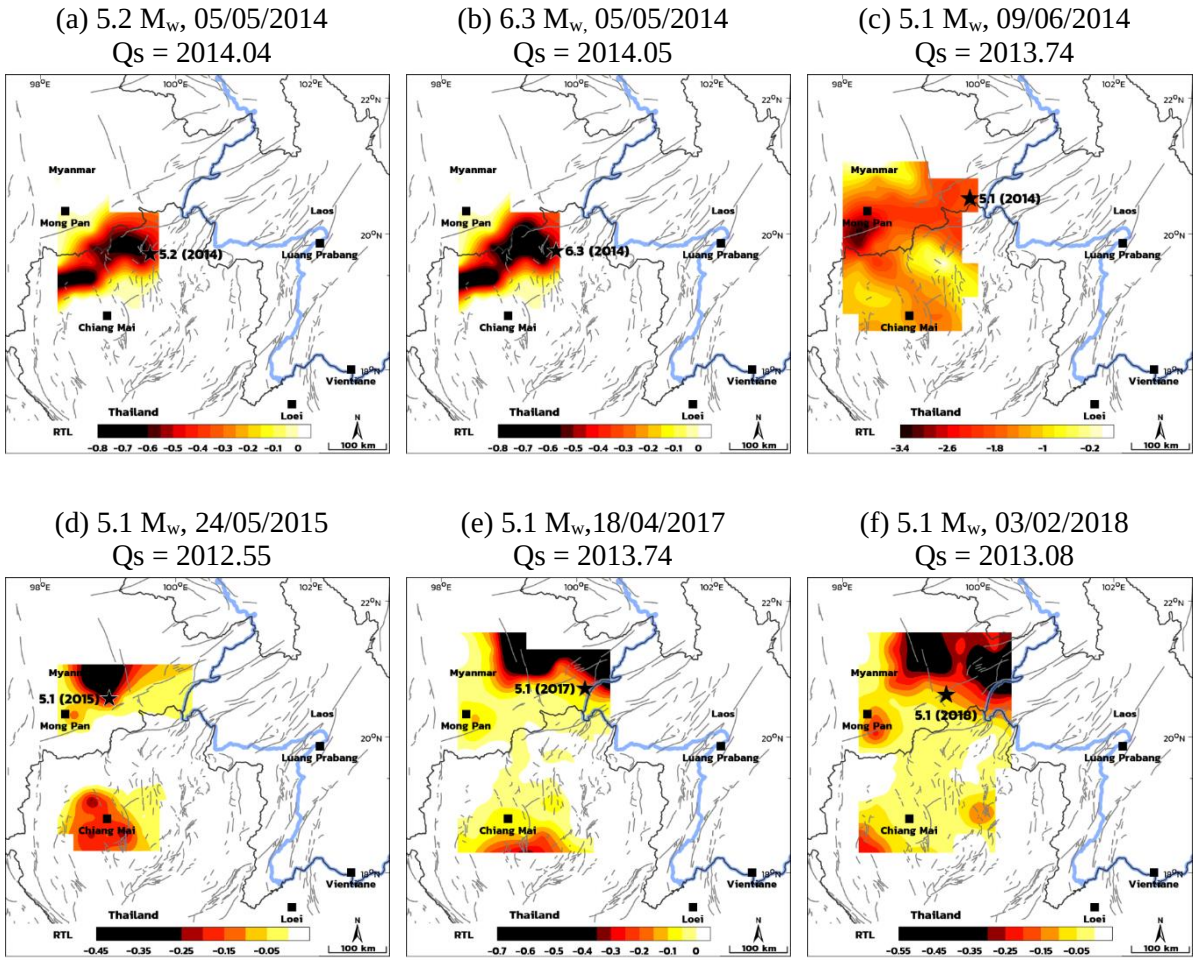

Figure 7. (a-f) indicates the spatial distribution of the RTL score during each case study's seismic quiescence (same six earthquakes as in Figure 6). The lower the RTL score, the less active the seismicity (quiescence) . The individual identified earthquake's epicenter is represented as a black star.

5. AN UPDATED PROSPECTIVE EARTHQUAKE SOURCE

To clarify the results of this research, the anomalous Z-value was compared to the anomalous RTL score. Additionally, it was observed that the seismicity rate varies in relation to seismic quiescence. Seismotectonically, the positive and negative Z-values correspond to the quiescence and activation stages, respectively, in the particular location and time period of interest. A lower RTL score, on the other hand, indicated a higher level of seismic quiescence. For instance, when the spatial distributions of the Z-value and RTL score are compared during the same time period in six occurrences, the places with a relatively high Z-value quite closely overlap to those with a low RTL score, shown in Figures 6a and 7a. The overlapping anomalous zones were primarily found north of Chiangmai, Thailand. As previously stated, two hazardous earthquakes occurred in this area on May 5th, 2014: the M_w-5.2 and M_w- 6.3 earthquakes. As a result, both the anomalous locations of the Z-value and RTL score, as well as the northern part of Chiang Mai, Thailand, the triple junction of the TLMB, and Mong Pan, Myanmar), may serve as precursors to the next upcoming earthquakes.

6. CONCLUSION

Precursory seismic quiescence, which is shown before strong-to-major earthquakes happen, was the goal of this study. It used the Z-value and RTL algorithm to find out more about it. The finding is beneficial for the contribution of a hazard map indicating the locations of potential earthquake-prone areas in the future. The following four conclusions are based on the results that were found.

(i) Using the most appropriate characteristic parameters for Z-value (N_w = 25 and T_w = 1.5) and the RTL algorithm (r_0 = 60 km and t_0 = 2.5), both methods can detect the seismic quiescence stage before the generation of thirteen and ten out of eight strong-to-major earthquakes, respectively.

(ii) The temporal investigation revealed that the time interval between the aforementioned quiescent stage and the occurrence of strong-to-major earthquakes was within the range of intermediate-term forecasting.

(iii) In this study, places with a relatively high Z-value corresponded to areas with a low RTL score

(iv) While the Z-value map illustrates a larger area of anomaly, the RTL algorithm map depicts a more precise region. Both techniques have the potential to forecast an upcoming earthquake.

7. ACKNOWLEDGEMENT

The author would like to express sincere gratitude to Advisor, all those, who helped in the entire study directly and indirectly for their constructive advisory and guidance knowledges. I acknowledge thoughtful comments and suggestions by the editors and anonymous reviewers that enhanced the quality of this manuscript significantly.

8. References

Bachmann D, (2001) Precursory seismic quiescence: Two methods of quantifying seismicity rate changes and an application to two Northern Californian mainshocks, Diploma Thesis's, Department of Earth Sciences of the Swiss Federal Institute of Technology, Zurich

Chen, C., Wu, Y., 2006. An improved region-time-length algorithm applied to the 1999 Chi-Chi, Taiwan earthquake, Geophys. J. Int.; 166, 144-147.

Chouliaras G (2009) Seismicity anomalies prior to 8 June 2008, Mw = 6.4 earthquake in Western Greece. Nat Hazard Earth Sys 9(2): 327-335

Gardner, J.K., Knopoff, L., 1974. Is the sequence of earthquakes in Southern California, with aftershocks removed, Poissonian?, Bulletin of the Seismological Society of America; 64(1), 363-367.

Habermann, R.E., 1983. Teleseismic detection in the Aleutian Island Arc, J. Geophys. Res.; 88, 5056-5064.

Habermann, R.E., 1987. Man-made changes of seismicity rates, Bull. Seismol. Soc. Am.; 77, 141-159.

Huang, Q., Oncel, A.O., Sobolev, G.A., 2002. Precursory seismicity changes associated with the M_w=7.4 1999 August 17 Izmit (Turkey) earthquake, Geophys. J. Int.; 151(1), 235-242.

Huang Q (2005) A method of evaluating reliability of earthquake precursors. Chin J Geophys 48(3):701-707Huang Q (2008) Seismicity changes prior to the Ms8.0 Wenchuan earthquake in Sichan, China. Geophys Res Lett 35: L23308

Huang Q, Ding X (2012) Spatiotemporal variations of seismic quiescence prior to the 2011 M 9.0 Tohoku Earthquake revealed by an improved region-time-length algorithm. Bull Seismol Soc Am 102(4):1878-1883

Huang Q, Nagao T (2002) Seismic quiescence before the 2000 M=7.3 Tottori earthquake. Geophys Res Lett 29(12):1578

Huang Q, Sobolev GA (2002) Precursory seismicity changes associated with

the Nemuro Peninsula earthquake, January 28, 2000. J Asian Earth Sci 21(2):135-146

Huang Q, Sobolev GA, Nagao T (2001) Characteristics of the seismic quiescence and activation patterns before the M=7.2 Kobe earthquake, January 17, 1995. Tectonophysics 337(1-2):99-116

Huang Q, Oncel AO, Sobolev GA (2002) Precursory seismicity changes associated with the Mw=7.4 1999 August 17 Izmit (Turkey) earthquake. Geophys J Int 151(1):235-242

Jiang, H.K., Hou, H.F., Zhou H.P., Zhou, C.Y., 2004. Region-time-length algorithm and its application to the study of intermediate-short term earthquake precursor in North China, Acta Seismol. Sin.; 17(2), 164-176.

Liu H, Su Y-J (2006) Application of region-time-length algorithm to Yunnan area. J Seismol Res 29(1):25–29

Katsumata K (2011) Precursory seismic quiescence before the Mw = 8.3 Tokachi-oki, Japan, earthquake on 26 September 2003 revealed by a re-examined earthquake catalog. J Geophys Res 116: B10307-1-16

Öztürk S, Bayrak Y, Precursory seismic quiescence before 1 May 2003 bing Öl (turkey) earthquake: A statistical evaluation. J Appl Funct Anal 4(4): 600-610

Pailoplee, S., Channarong, P., and Chutakosikanon, V., 2013. Earthquake Activities in the Thailand-Laos-Myanmar borders: A Statistical Approach, Terr. Atmos. Ocean. Sci.; 24(4), 721-730.

Puangjaktha, P., Pailoplee, S. (2016). Evolution of Precursory Seismic Quiescence of the Mw-6.8 Nam Ma Earthquake, Thailand-Myanmar Borders. Bulletin of Earth Sciences of Thailand, 7, 1-15.

Pailoplee S, Choowong M (2014) Earthquake frequency-magnitude distribution and fractal dimension in mainland Southeast Asia, Earth Planets Space 66(1):1-10.

Rudolf-Navarro AH, Muñoz-Diosdado A, Angulo-Brown F (2010) Seismic quiescence patterns as possible precursors of great earthquakes in Mexico. Int J Phys Sci 5(6): 651-670

Sobolev, G.A., 1995. Fundamental of Earthquake Prediction Electromagnetic Research Center, Moscow, 162 pp.

Sobolev, G.A., Tyupkin, Y.S., 1997. Low-seismicity precursors of large earthquakes in Kamchatka, Volc. Seismol.; 18, 433-446.

Sobolev, G.A., Tyupkin, Y.S., 1999. Precursory phases, seismicity precursors, and earthquake prediction in Kamchatka, Volc. Seismol.; 20, 615-627.

Sorbi MR, Nilfouroushan F, Zamani A (2012) Seismicity patterns associated with the September 10th, 2008 Qeshm earthquake, South Iran. Int J Earth Sci 101(8): 2215-2223

Wang Y, Lin YNN, Simons M, Tun ST 2014 Shallow rupture of the 2011 Tarlay earthquake (Mw 6.8), eastern Myanmar. Bull Seismol Soc Am 104(6): 1-10.

Wiemer, S., Wyss, M., 1994. Seismic quiescence before the Landers M=7.5 and Big Bear M=6.5 1992 earthquakes. Bulletin of the Seismological Society of America 84, 900-916.

Woessner, J., Wiemer S., 2005. Assessing the Quality of Earthquake Catalogues: Estimating the Magnitude of Completeness and Its Uncertainty, Bull. Seismol. Soc. Am.; 95(2), 684-698.

Zuniga, F.R., Wiemer, S., 1999, Seismicity patterns: are they always related to natural causes. Pageoph; 155, 713-726.